Microchemical Journal 181 (2022) 107844

Contents lists available at ScienceDirect

Microchemical Journal

journal homepage: www.elsevier.com/locate/microc

A statistical interpretation of the voltammetry of adsorbed substances under the perspective view of the Digital Video Electrochemistry

Jerónimo Agrisuelas, José Juan García-Jareño *, Francisco Vicente

Physical-Chemistry Department, University of Valencia, Dr. Moliner 50, 46100 Burjassot, Spain

ARTICLE INFO

Keywords:
Cyclic voltammetry
Digital Video Electrochemistry
Color efficiency
Surface color
Dispersion
Thin films

ABSTRACT

Coupling cyclic voltammetry with digital video electrochemistry allows identifying different electrochemical processes overlapped. Mathematical description of the time evolution of mean color intensities and their standard deviation at the studied electrode surface during voltammetric experiments were developed. Parallel electrochemical reactions and the presence of colored intermediate species was also evaluated. Single expressions for the shape of these curves, including the maximum of peaks or the half-peak widths are analyzed on the basis of a single layer covered electrode. The good similitude among current, mean color intensities derivative and variance curves allows a statistical interpretation for these processes.

1. Introduction

The analysis of experimental data obtained by electrochemical techniques can give rich information on the studied system. Electrochemical techniques are always a fast way for a plethora of electroanalytical applications, including electrochemical sensing, corrosion detection, mechanistic investigations, or catalysis [1]. One of the most used techniques for describing electrochemical processes is undoubtedly linear sweep voltammetry (LSV) or cyclic voltammetry (CV) [2–4]. This technique allows identifying different electrochemical processes by the potential at which they exchange electrons, but also allows obtaining kinetic parameters from the shape of the obtained voltametric peaks - the current–potential waveform obtained. Some measurements related with these kinetic parameters are peak heights, peak widths or half peak widths and peak to peak separation. One particular case of LSV is for adsorbed electroactive species. Assuming that there is no mass transport control, and that both, the oxidized and the reduced species keep on the electrode surface, there are simplified equations describing the shape of these curves[5]. These equations are obtained from theoretical models introducing different approaches to the real behavior of these systems, such as it could be non-interaction between active centers, the homogeneous electrode surface, thin films where the transport of electroactive species does not affect the measured current, reversible processes or that capacitive currents are not considered [1,5]. Nevertheless, in non-ideal conditions theoretical models proved more complicated [6,7].

However, the chemistry of the electrode–electrolyte interface is still not fully understood, particularly in electrochemical complex systems. For this reason, the advanced electrochemical techniques coupling classical electrochemical techniques with spectroscopical or electrogravimetric techniques have revealed as a powerful tool for the knowledge of kinetics in different systems [8–14]. One particular case for adsorbed species is the CV experiment for conducting polymers [15–18]. Apart from current, there are also changes in mass during redox processes detected by the electrochemical quartz crystal microbalance (EQCM). Based on an insertion model, redox processes of a polymer can be schematized by:

$$< P > + ne^- + nM^+ \rightleftarrows < P(red), nM^+ > \quad (1)$$

$$< P, nA^- > + ne^- \rightleftarrows < P(red) > + nA^- \quad (2)$$

where the electric charge during redox processes is balanced by the exchange of anions (A^-) and/or cations (M^+). In these cases, if only one ion is exchanged during the redox process, and there is a stoichiometric relation between active centers reduced and the number of ions exchanged, mass changes are related with the electric current by:

$$\frac{dq}{dt} = i = n_e F \frac{dn_a}{dt} \quad (3)$$

where n_e is the number of involved electrons, F is the Faraday constant and n_a is the number of oxidized electroactive sites. Then, for a reduction process n_a decreases and a negative current is measured, while the

* Corresponding author.
E-mail address: Jose.J.Garcia@uv.es (J.J. García-Jareño).

https://doi.org/10.1016/j.microc.2022.107844
Received 13 June 2022; Received in revised form 28 July 2022; Accepted 29 July 2022
Available online 1 August 2022

opposite occurs for an oxidation process. The mass increase or decrease for the exchange of one ion is given by:

$$\frac{dm}{dt} = -\frac{M}{z} n_e \frac{dn_a}{dt} \tag{4}$$

where z is the electric charge of the ion and M its molar mass. Then, the ratio between mass changes and electrical charge is given by [19],

$$F\frac{dm}{dq} = -\frac{M}{z} \tag{5}$$

The minus sign appears since mass increases during the cathodic process (negative current) by the insertion of cations, and the opposite occurs during the anodic process. If more than one species is exchanged this value is displaced from the expected one for the ideal case. This is an example of how a single calculation can give an extra information about the role of different species during the redox process identifying the molar mass of the exchanged species (Scheme 1).

If, in addition, the conducting polymer provides color changes during the oxidation–reduction conversions (spectroelectrochemical experiments), the measured absorbance can be related with the number of active centers by the Beer's law, and the derivative of absorbance with the measured current [20–23]. In this case, the ratio between absorbance derivative and measured current is related with the molar absorptivity (ε) of the different active centers [24].

$$A = \varepsilon l \frac{n_a}{V} \tag{6}$$

$$\frac{dA}{dt} = \frac{\varepsilon l}{V}\frac{dn_a}{dt} \tag{7}$$

where V is the film volume and l is the optic path length (Scheme 2).

In all three cases, the waveform of dq/dt, dm/dt and dA/dt against the potential should be similar if there is only one electroactive process with one ion exchange participation and color switching. In some cases, dA/dt or dm/dt curves show more than one peak where only one voltametric peak was observed indicating that this current peak involves complex processes with the participation of intermediate species (consecutive reactions) or simultaneous reactions (parallel reactions). If these color and mass changes are recorded and quantified, they prove a good measure of the chemical reaction advance as the *in situ* spectroelectrochemistry and electrogravimetry reveal for thin-layer electrogenerated species [11,25–29].

However, these techniques require, among many other things, absence of light for the spectroscopy or special resonant electrodes for the EQCM case, where not always correspond to the experimental conditions for a normal use of the electrochemical system. Another important fact is that spectroscopical techniques and gravimetric ones are usually designed for small electrodes at the laboratory scale. Usually during an electrochemical experiment current and mass are globally measured, and spectroscopy (Absorbance) corresponds to a small region on the electrode surface, but these techniques do not allow measuring simultaneously and independently what happens on the entire electrode and on any part on the electrode surface in a synchronous way. There are some equipment allowing local measurements of impedance (local impedance) [30,31] or absorbance at more than one point on the electrode [32], but a large number of regions on the surface at the same time is not possible for now.

For the surface studies, an ideal method should be able to give a fast and accurate response of the chemical reaction advance at each point on the active surface. During the last few years, digital video-electrochemistry (DVEC) has revealed as both, a non-expensive way to obtain spectroelectrochemical data of different systems but also an excellent tool to get spatiotemporal information of the entire surface of the electrode independently of the electrochemical technique used [33–38]. This brand-new technique solves partially the above-mentioned issues allowing to work in similar or identical experimental conditions during the normal operation of many processes if light conditions remain constant. In addition, DVEC has no requirement about the transparency, reflectivity or size of the electrode allowing at the same time recording global information of the whole piece, but also local information at any part on the studied piece by selecting it for the video analysis. DVEC has allowed synchronous studies of electrodeposition of metals on resistive materials at different parts on the electrode surface [37], having a good estimation of the different covering rate and more recently synchronous studies of local color impedance at different parts on the electrode surface [38]. As a complementary and alternative tool, the analysis of digital images allows to investigate the kinetics on the entire surface of different substrates [39–44].

$$A_1 + e^- + M^+ \rightarrow B \qquad (E_1^{0'})$$

$$A_2 + e^- + M^+ \rightarrow C \qquad (E_2^{0'})$$

Scheme 1. Electrochemical parallel reactions mechanism. A_1 (70%) and A_2 (30%) refer to different active centers on the electrode surface.

$$A + e^- + M^+ \rightarrow In \qquad (E_1^{0'})$$

$$In + e^- + M^+ \rightarrow B \qquad (E_2^{0'})$$

Scheme 2. Electrochemical consecutive reactions mechanism. *In* refers to an intermediate specie.

The main objective of this research is to evaluate the use of digital video-electrochemistry for the interpretation of voltammetry of thin layers such as electrochromic polymers which can be used in different electrochemical sensors. For that purpose, mathematical models based on statistical of color changes on the electrode surface were developed.

2. Material and methods

To obtain good quality data from DVEC, digital video should be acquired under controlled light conditions configurating accurately the digital video acquisition. Among others, these parameters should be kept constant during video acquisition: external light, white balance, exposition, and frame rate. The video camera and the studied surface should be fixed for a correct data comparison. These experimental conditions can be extrapolated, for example, in an industrial production process since they allow to follow the time evolution of different surfaces under operating conditions.

After video acquisition, each image frame is obtained separately and then, the portion of the surface to be studies could be cropped from the original picture. From these images, red, green and blue color intensities (I_R, I_G, I_B) values at each pixel are extracted and then mean color intensities ($\bar{I}_R$, $\bar{I}_G$ and $\bar{I}_B$) and the standard deviation (sd_R, sd_G and sd_B) are mathematically estimated from the corresponding histogram of the cropped image by equations (8) and (9). Fig. 1 shows a schema of the experimental setup needed to obtain valuable video-electrochemistry data. More details about how to obtain and how to manage video-electrochemistry data can be consulted in recent works [33,34,37,45].

All electrochemical experiments were carried out in a typical three electrodes cell. Auxiliary electrode was a Pt mesh, the reference electrode was the Ag|AgCl|KCl (0.5 M) which all potentials are referred to. The cell was a square cell made of optical glass (2 cm × 2 cm). Digital video (30 fps) was recorded with a digital camera (EPA-503278). All the experiments were made in a 'home made' white box illuminated with LED strips (6500 K, 10 W). All experiments were controlled with a PAR 273 A potentiostat–galvanostat.

Prussian Blue films (PB) were electrogenerated on 1 cm^2 ITO electrodes by applying a controlled cathodic current of 40 $\mu A\ cm^{-2}$ for 150 s (electric charge of 6 mC cm^{-2}) in a 0.02 M $FeCl_3$, 0.02 M $K_3Fe(CN)_6$ and 0.01 M HCl [46,47]. After electrodeposition, these films were stabilized

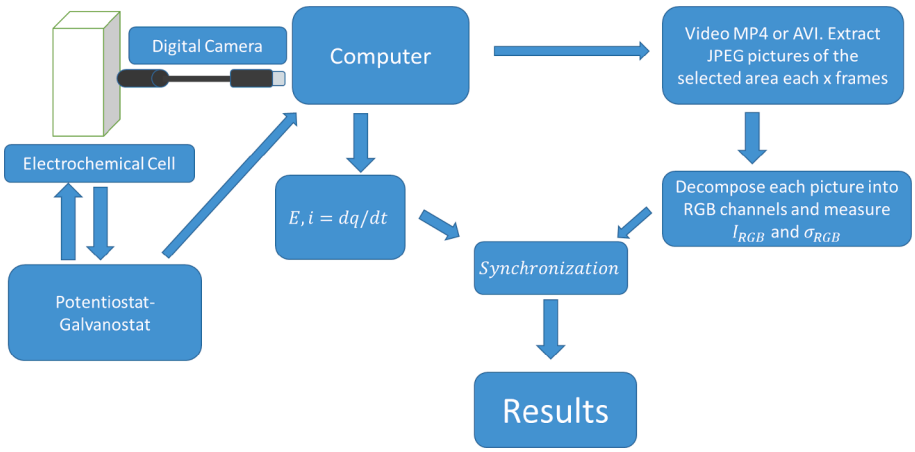

Fig. 1. Schema of Digital Video Electrochemistry (DVEC) technique.

by cyclic voltammetry in a 0.5 M *KCl* solution in the potential range between 0.6 V and −0.2 V against the reference electrode until a stable voltammogram was recorded [47].

Poly (methylene-blue) (PMB) was electrogenerated by cyclic voltammetry between −0.4 V and 1.1 V against the Ag|AgCl|KCl (0.1 M) reference electrode at 20 $mV\,s^{-1}$ and for 10 cycles in a methylene-blue monomer solution 20 mg/100 mL of KCl 0.1 M at pH = 9 adjusted by addition of KOH. As a result, the electrogenerated film was a dark blue film on the transparent ITO electrode, however, the amount of electrogenerated polymer was not possible to quantify [48]. All reagents were A.R. grade from Scharlau except the methylene blue monomer which was supplied by Fluka and no extra purification was made. Electrogenerated PMB films were studied by cyclic voltammetry in a 0.5 M KNO_3 solution at different scan rates in the range of potentials between −0.4 V and 0.5 V against the Ag|AgCl|KCl (0.5 M) reference electrode.

3. Theory and methodology

Among others, two characteristics made of Digital Video Electrochemistry (DVEC) an ideal technique to be successfully implemented with electrochemical ones. On the one hand, DVEC takes advantage of a fast image acquisition rate (30 fps or more) to unravel fast electrochromic processes taking place on the electrode surface [33,34,37,45,49]. On the other hand, DVEC proves enough resolution to distinguish between different surface colors and/or different substances on the surface in many cases.

Video is converted into separated and sequential images. Each acquired image is decomposed into individualized pixels characterized by red, green, and blue intensities coordinates (I_R, I_G and I_B), which are intuitively related with spectroscopic parameters such as light intensity at a given wavelength or their corresponding absorbance: the RGB colors supply transmitted spectroscopic information about 650 nm, 510 nm, and 475 nm wavelengths, respectively [45,50]. As an example, in a classical 24-bit digital image, color intensity for each color has an 8-bits resolution. That means $2^8 = 256$ color intensity levels (0: black, 255: pure color) for each coordinate giving a result of $2^{24} = 16777216$ combinations, in other words, it provides information of the whole visible spectrum.

Furthermore, the singular characteristic of DVEC is the analysis of the color intensities evolution at each point on the surface and at any time making possible the spatiotemporal study of the system [45]. Therefore, we can obtain specific kinetics on any part of the studied surface. It should be considered that homogeneous surface electrodes are only possible as an ideal situation. In real electrochemical systems, the non-uniform surface causes the rate of electrochemical processes to be different on different parts on the surface. In some cases, there is also a gradient of a physical property such as it could be the ohmic drop causing a different behavior depending on the distance from the electrical contact [17,37,45,51]. That could represent an interesting advance studying kinetics for non-homogeneous surfaces since it is possible analyzing the chemical advance simultaneously on different parts once the electrochemical assay is recorded.

The analysis of each digital image captured during an electrochemical experiment implies managing a large amount of data. Initially, this was a handicap in the analysis of the chemical or physical processes taking place on the studied surface and their correlation with the physical or chemical evolution of the studied system. A smart strategy was to reduce the amount of information to easily interpretable parameters. From a practical point of view, distribution of the color intensity into the pixel matrix of the studied surface image can be represented as a histogram and characterized by a mean color intensity ($\bar{I}_R$, $\bar{I}_G$ or $\bar{I}_B$) and their standard deviation (sd_R, sd_G or sd_B) for each color coordinate.

For the simplest case, let us assume that each pixel on the electrode surface is related with an active center, then the mean color intensity of a region on the electrode surface (i.e. a matrix of pixels) should be given by:

$$\bar{I} = \sum_i^{n_p} \frac{I_i}{n_p} \tag{8}$$

In this expression, n_p is the number of pixels of the selected surface of the studied image, I_i is the color intensity of R, G or B coordinates of the i^{th} pixel and $\bar{I}$ is the mean color intensity for the R, G or B coordinate. For the case where the pixel size was larger than the size of the active center, each pixel will recover the information of a group of active centers and the mean color intensity will not be affected.

The standard deviation of each color coordinate (sd_R, sd_G and sd_B) measures dispersion or distribution of color intensity for each RGB coordinate of the pixelated image and is estimated as:

$$\mathrm{sd} = \sqrt{\sum_i^{n_p} \frac{(I_i - \bar{I})^2}{n_p}} \tag{9}$$

In a homogeneous surface the distribution of oxidized and reduced centers should be the same independently of the studied region on the electrode surface, therefore the values of the standard deviation of color intensity should be identical for homogeneous surfaces at any part on the studied surface. In recent works, our group has related this parameter with kinetics of the surface processes during the color changes of an electrochromic polymer and in copper electrodeposition on composite electrodes [34,35,37]. In view of these promising results, the aim of this work is to extend the interpretation of the time evolution of standard deviation and color intensity derivative curves during classical electrochemical experiments as the cyclic voltammetry. The waveform of

standard deviation and mean color intensity time-derivatives ($d\bar{I}/dt$) curves, the maximum of peaks or the half-peak widths depends on the nature of the studied process, but also on the experimental conditions.

3.1. DVEC in voltammetry for adsorbed species.

Even assuming an ideal homogeneous surface, not all the electroactive centers reduce or oxidize simultaneously during a voltammetry sweep. Theoretical models predict a potential window where changes of oxidation state take place. A statistical interpretation can be inferred, supposing all centers have the same probability to evolve, the applied potential during a voltametric experiment changes the probability factor for each center. Thus, at a given potential the number of active centers that have evolved are related with this probability. If active centers present different color if oxidized or reduced, the measure of color surface proves an excellent way to know the ratio between oxidized and reduced centers.

3.1.1. Single reaction

Now, let us consider the simplest case of a homogeneous surface where color changes are due to a chemical or physical process and go from color (1) characterized by the RGB intensity coordinates (I_1) to color (2) characterized by the RGB intensity coordinates (I_2). If this applies independently of the analyzed color coordinate, equations (8) and (9) can be rewritten as.

$$\bar{I} = \frac{n_1 I_1 + n_2 I_2}{n_p} \tag{10}$$

$$sd = \sqrt{\frac{n_1 (I_1 - \bar{I})^2 + n_2 (I_2 - \bar{I})^2}{n_p}} \tag{11}$$

where n_1 and n_2 are the number of pixels with I_1 and I_2, respectively.

As there are only two possible colors for this simplified case, the sum of pixels with I_1 and I_2 is the number of pixels of the full image (n_p). Intuitively, sd should be 0 if the entire surface has the same intensity coordinate (I_1 or I_2), therefore, larger values are expected for intermediate situations with a maximum according to the Rolle's theorem.

Substituting $\bar{I}$ from equation (10) into equation (11), we obtain for the variance [35]:

$$sd^2 = (I_2 - I_1)^2 \frac{n_1 (n_p - n_1)}{n_p^2} \tag{12}$$

then, differentiating the equation (12) and equaling to zero, sd^2 is maximum if:

$$n_1 = \frac{n_p}{2} = n_2 \tag{13}$$

The time when sd^2 is maximum corresponds to the time when one half of surface is I_1 and the other half is I_2. Substituting this maximum condition into equation (12), we arrive at the maximum standard deviation value when.

$$sd^2_{max} = \frac{(I_2 - I_1)^2}{4} \tag{14}$$

During a voltametric experiment, we assume that kinetic constants associated to the redox processes of electroactive species are potential dependent, and they should vary during the potential scan. If no mass control applies, as a first approach, one can assume that the rate of the process is controlled by the potential on the electrode surface (E) where the ratio between surface concentrations of reduced and oxidized species (Γ_{red}/Γ_{ox}) is given by the Nernst equation for a reversible process [1,15,17].

$$E = E^{0'} - \frac{RT}{nF} \ln\left(\frac{\Gamma_{red}}{\Gamma_{ox}}\right) \tag{15}$$

This is a common assumption for electroactive processes of adsorbed species. If we assume that I_1 corresponds to the color for the reduced form and I_2 for the oxidized one, and we consider that there are n_1 reduced centers and $n_2 = n_p - n_1$ oxidized centers, then equation (15) becomes:

$$E = E^{0'} - \frac{RT}{nF} \ln\left(\frac{n_1}{n_p - n_1}\right) \tag{16}$$

Therefore, the potential dependence of the number of pixels with color I_1 (n_1) is given by:

$$n_1 = \frac{n_p}{e^{b(E - E^{0'})} + 1} \quad \text{where} \quad b = \frac{nF}{RT} \tag{17}$$

n is the number of electrons involved, R is the gas constant and T the temperature.

During the voltametric experiment the applied potential changes with the time according to:

$$E = E_s + \nu t \tag{18}$$

where E_s represents the starting potential and ν the scan rate. Substituting equation (17) and equation (18) into equation (10), we obtain for the mean color intensity:

$$\bar{I} = \frac{\frac{n_p}{e^{b(E - E^{0'})}+1} I_1 + \left(n_p - \frac{n_p}{e^{b(E - E^{0'})}+1}\right) I_2}{n_p} = \frac{I_2 e^{bvt + E_s b} + I_1 e^{E^{0'} b}}{e^{bvt + E_s b} + e^{E^{0'} b}} \tag{19}$$

and differentiating,

$$\frac{d\bar{I}}{dt} = \frac{(I_2 - I_1) bv e^{(bvt + E_s b + E^{0'} b)}}{\left(e^{(bvt + E_s b)} + e^{(E^{0'} b)}\right)^2} \tag{20}$$

This equation can be rewritten by dividing both, numerator and denominator, by $e^{2bE^{0'}}$:

$$\frac{d\bar{I}}{dt} = (I_2 - I_1) bv \frac{e^{b(E_s + \nu t - E^{0'})}}{\left(1 + e^{b(E_s + \nu t - E^{0'})}\right)^2} \tag{21}$$

On the other hand, and for variance curves assuming equation (17) and substituting into equation (12), we obtain:

$$sd^2 = (I_2 - I_1)^2 \frac{e^{b(E_s + \nu t - E^{0'})}}{\left(1 + e^{b(E_s + \nu t - E^{0'})}\right)^2} \tag{22}$$

For current, it is the well-known equation for adsorbed species and only one reversible process and controlled by the electron transfer step [1,2,5,17]:

$$i = \frac{n^2 F^2 \nu A \Gamma_0}{RT} \frac{e^{b(E_s + \nu t - E^{0'})}}{\left(1 + e^{b(E_s + \nu t - E^{0'})}\right)^2} = nFA\Gamma_0 bv \frac{e^{b(E_s + \nu t - E^{0'})}}{\left(1 + e^{b(E_s + \nu t - E^{0'})}\right)^2} \tag{23}$$

where Γ_0 is the surface concentration of electroactive centers ($\Gamma_{red} + \Gamma_{ox}$).

These expressions can be simplified if the following change is considered:

$$\frac{e^{b(E_s + \nu t - E^{0'})}}{\left(1 + e^{b(E_s + \nu t - E^{0'})}\right)^2} = \frac{1}{4\cosh^2\left(\frac{b}{2}\left(E_s + \nu t - E^{0'}\right)\right)} \tag{24}$$

therefore, equations (21), (22) and (23) can be rewritten proving the obviously similitude among them:

$$\frac{d\bar{I}}{dt} = \frac{bv(I_2 - I_1)}{4\cosh^2\left(\frac{b}{2}\left(E_s + \nu t - E^{0'}\right)\right)} \tag{25}$$

$$sd^2 = \frac{(I_2 - I_1)^2}{4\cosh^2\left(\frac{b}{2}\left(E_s + \nu t - E^{0'}\right)\right)} \tag{26}$$

$$\mathrm{i} = \frac{nFA\Gamma_0 b\nu}{4\cosh^2\left(\frac{b}{2}\left(E_s + \nu t - E^{0'}\right)\right)} \tag{27}$$

Characteristically, maximum of each equation is achieved if potential is $\mathrm{E} = E_s + \nu t = E^{0'}$ and then, $\cosh^2\left(\frac{b}{2}\left(E_s + \nu t - E^{0'}\right)\right) = 1$:

$$\left(\frac{d\bar{I}}{dt}\right)_{max} = b\nu\frac{(\mathrm{I}_2 - \mathrm{I}_1)}{4} \tag{28}$$

$$sd^2_{\max} = \frac{(I_2 - I_1)^2}{4} \tag{29}$$

$$i_{max} = \frac{nFA\Gamma_0 b\nu}{4} \tag{30}$$

For the mean color intensity peak equation (28), the peak height value depends linearly on the scan rate and this peak can reach negative or positive values depending on the difference between I_2 and I_1 and the sign of the scan rate. For the current (equation (30)), the peak height proves positive for the anodic scan ($\nu > 0$) and negative for the cathodic one. Notably looking now at equation (29), one can observe that maximum values of variance are not associated to the scan rate, nor to the number of electrons or temperature. It only depends on the color difference between the reduced and oxidized forms $(I_2 - I_1)^2$, and obviously, maximum values are always positive.

According to equations (28) and (29) it proves immediate obtaining the number of electrons involved in the electrochemical process by:

$$\frac{\left(\frac{d\bar{I}}{dt}\right)_{max}}{sd_{max}} = \frac{b\nu\frac{I_2 - I_1}{4}}{\frac{I_2 - I_1}{2}} = \frac{b\nu}{2} = \frac{nF}{2RT}\nu \tag{31}$$

Other interesting factor in the voltametric peaks analysis is the half-peak width ($\omega_{1/2}$) study. In all three cases, we obtain the same expression for $\omega_{1/2}$:

$$\omega_{1/2} = 3.526\frac{RT}{nF} = \frac{90.5}{n}(mV\ at\ \ 298\ K) \tag{32}$$

Therefore, this parameter depends on the number of electrons involved in the electron transfer reaction independently of the analyzed parameter. In this last case, working with different color intensities or variances can allow to obtain individual information for overlapped processes.

Fig. 2 collects a set of CV simulations at different scan rates illustrating these observations. For this case where current and the color intensity are directly related, peak currents and the height of $d\bar{I}/dt$ peaks proved both proportional to the scan rate, however, variance peaks keep unaltered.

In this case, we can estimate an apparent electromonochromatic coefficient (in mol^{-1}), like the molar absorptivity but directly related with one color intensity. This parameter can be obtained by the expression:

$$F\left(\frac{d\bar{I}}{dq}\right) = \mathrm{F}\left(\frac{d\bar{I}/dt}{\mathrm{dq/dt}}\right) = \mathrm{F}\left(\frac{d\bar{I}/dt}{\mathrm{i}}\right) \tag{33}$$

and introducing eqs. (21) and (23) we arrive at:

$$F\left(\frac{d\bar{I}}{dq}\right) = \frac{I_2 - I_1}{nA\Gamma_0} \tag{34}$$

For a system with only one process, this parameter should keep constant during the voltametric peak. On the contrary, a transition between different values is expected for a multi-process system. This kind of electrochromic efficiencies can be used for the current peaks deconvolution in multi-process systems [24,45,50].

A new interpretation for voltammetric curves of adsorbed species could be inferred from these equations. The good correlation among equations (25), (26) and (27) clearly indicates that current is directly related with the dispersion of active centers on the electrode surface and also on the color intensity derivative curves. We can easily obtain at any time or potential:

$$\frac{sd^2}{i} = \frac{RT}{n^2F^2}\hat{\mathrm{A}}\cdot\frac{(I_2 - I_1)^2}{\nu A\Gamma_0} = \frac{(I_2 - I_1)^2}{nFb\nu A\Gamma_0} \tag{35}$$

$$\frac{dI/dt}{i} = \frac{\mathrm{I}_2 - \mathrm{I}_1}{nFA\Gamma_0} \tag{36}$$

$$\frac{sd^2}{dI/dt} = \frac{I_2 - I_1}{b\nu} \tag{37}$$

These equations can be very useful for deconvolution of overlapped

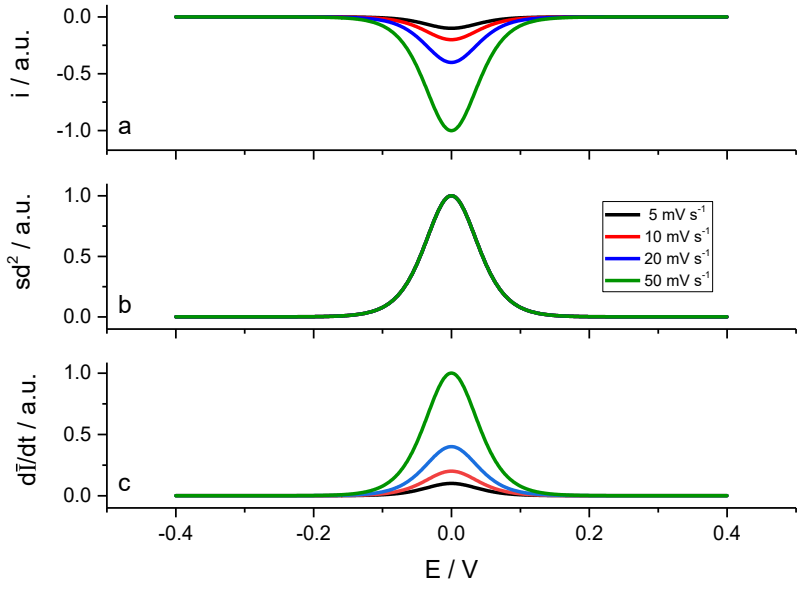

Fig. 2. Simulated current (a), variance (c) and color intensity derivative (c) changes during a voltammogram of a single reaction. Y-axis is normalized to the highest value. Scan rates simulated are 5 mV s^{-1}, 10 mV s^{-1}, 20 mV s^{-1} and 50 mV s^{-1}.

processes, since current associated to each process is proportional to the sd^2. For a multi-process system where red, green and blue colors are associated to different electrochemical processes, from their variance or dI/dt evolution against time it could be possible to separate the different contributions to the overall current process. Therefore, the well-known equation for current against potential during a voltametric experiment of adsorbed species (Equation (27)) could also be interpreted as a measure of the dispersion or variance of the reduced or oxidized active centers on the electrode surface. The advantage of measuring color evolution and variance evolution together with the current against the potential is that it could be possible to discern and to separate electrochromic processes from another overlapped chemical or electrochemical reaction involving current but not color changes. Some experimental results can be explained according to this model, as for example the time evolution for standard deviation of red and blue colors for chronoamperometry of Prussian Blue films [34].

3.1.2. Multiple parallel reactions

One sample of a multi-process system could be the interconversion of one electrochromic center into two species characterized by different colors. This is a parallel or competitive electrochemical reactions case (schema (1)). Fig. 3 collects simulations for different situations in a 2 processes system. Some inorganic materials as Prussian Blue can show different active centers due to the neighboring atoms or vacants and could be an example of this case [8,17,52]. If we assume that both active centers A_1 and A_2 have the same original color (color 1) but after reduction they show a different color:

In this example, it is considered that 70 % of the active centers correspond to the A_1 species and evolve to color 2 (specie B) and the A_2 (30 %) can evolve to color 3 (specie *C*). In all three simulated cases there are only changes in the color intensity of the oxidized and reduced species and therefore current curves are always the same. However, variance and color intensity derivative depend on the electrochromic parameters.

Fig. 3 shows simulations of different parameters assuming parallel reactions. These simulations were obtained with wx-Maxima software. Current and surface concentrations curves were obtained considering that both are Nernstian processes. Then, analytical expressions for the number of centers with color 1, 2 and 3 as a function of the applied potential are obtained. Finally, these expressions were introduced in theoretical expressions for the mean color intensity and standard deviation (see supplementary material for more information).

Current shows a double peak system since electrode processes are quite separated in potential (0.28 V and 0.10 V). The largest one is for the 0.10 V peak since 70 % of the electrode surface is occupied by active centers that follow this process. The case of the $d\bar{I}/dt$ curves a double peak is also observed, but the height of the peaks is not only affected by the concentration factor, but also by the electrochromic efficiency for each one of the processes, or in other words, by the difference between the oxidized and reduced colors of the active centers. Then, peaks can be positive or negative. Variance curves can show a peak if the final color for the reduced centers proves similar to the initial one, but if these are very different colors, the reduced form can show a high value of variance, but no maximum is reached at intermediate potentials.

3.1.3. Consecutive reactions

Other example of multi-system process consider that intermediate species appear during consecutive reactions (schema (2)). Fig. 4 collects some simulations for this kind of electrochemical process in two steps.

For this simulation, it is supposed that the ratio between intermediate *In* and *A* is given by the Nernst law with a formal potential $E_1^{0'}$, also the ratio between *B* and *In*, but in this case with a formal potential $E_2^{0'}$. It is also considered that the number of active centers on the electrode surface keeps constant during the experiment. For simulations in Fig. 4, we use wx-Maxima software to obtain an analytical expression for the number of centers with color 1, 2 and 3 against the applied potential considering that the Nernst equation applies for consecutive electrochemical reactions. Then, we obtain an expression for the mean color intensity and variance at each potential (see supplementary material for more information).

In Fig. 4, the characteristic colors of *A* and *B* are similar and the intermediate specie shows a large color difference. Simulation 1 corresponds to the case where both formal potentials are near. In this case, current shows a wider voltametric peak, standard deviation shows also a wider peak and $d\bar{I}/dt$ shows a characteristic increase–decrease shape which indicates appearance of the intermediate and then, disappearance

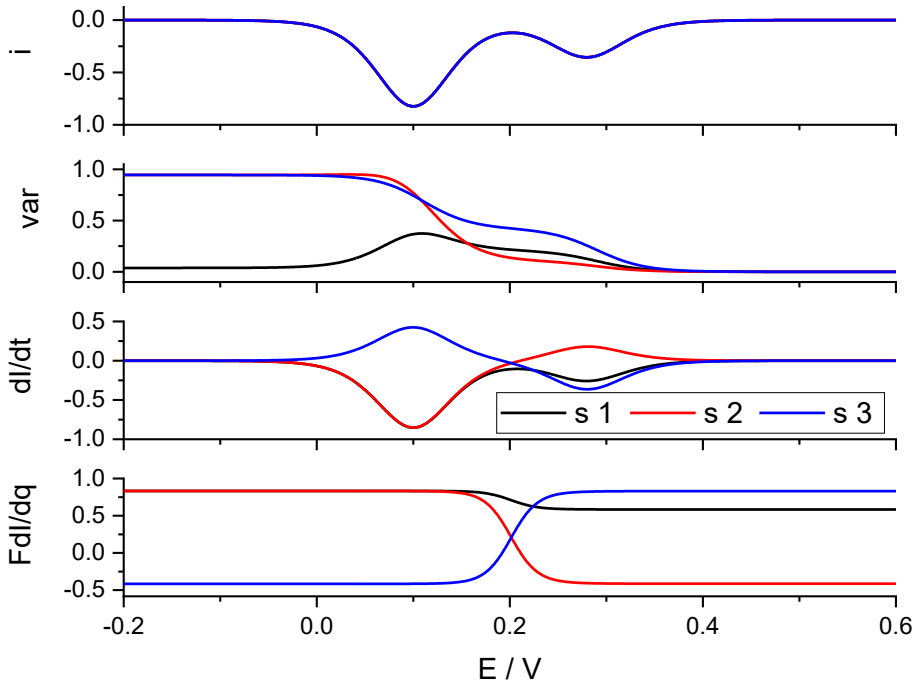

Fig. 3. Simulation of parallel reactions. Simulated current (a), variance (b), color intensity derivative (c) and FdI/dq (d) changes during a voltammogram with multiple parallel reactions (schema (1)). Y-axis is normalized to the highest value. Parameters for the simulated curves: Process 1: 70 %, process 2: 30 %, $E_1^{0'} = 0.1V$, $E_2^{0'} = 0.28V$ are defined in schema (1). Simulation 1: $I_1 = I_2 = 150$, $I_{F1} = 50$, $I_{F2} = 80$, Simulation 2: $I_1 = I_2 = 150$, $I_{F1} = 50$, $I_{F2} = 200$, Simulation 3: $I_1 = I_2 = 150$, $I_{F1} = 200$, $I_{F2} = 50$. I_1 *and* I_2 are the characteristic color for the active centers '1' and '2' before reaction, I_{F1} *and* I_{F2} are the characteristic colors for the active centers '1' and '2' after reaction.

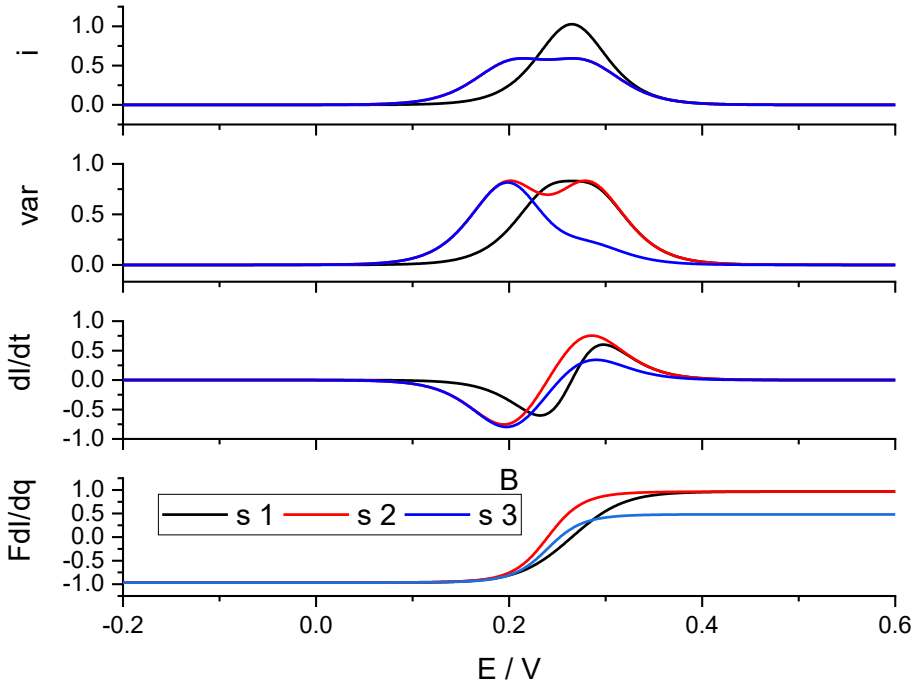

Fig. 4. Simulated current (a), variance (b), color intensity derivative (c) and FdI/dq (d) changes during a voltammogram with consecutive reactions (schema (2)). Y-axis is normalized to the highest value. Parameters for the simulated curves: Simulation 1: $E_1^{0'} = 0.25V$, $E_2^{0'} = 0.28V$, $I_1 = 50$, $I_2(intermediate) = 150$, $I_3 = 50$ Simulation 2: $E_1^{0'} = 0.20V$, $E_2^{0'} = 0.28V$, $I_1 = 50$, $I_2(intermediate) = 150$, $I_3 = 50$ Simulation 3: $E_1^{0'} = 0.20V$, $E_2^{0'} = 0.28V$, $I_1 = 50$, $I_2(intermediate) = 150$, $I_3 = 100$. I_1 *and* I_3 are the characteristic color for the active centers before and after reaction. I_2 is the characteristic color for the intermediate. $E_1^{0'}$ *and* $E_2^{0'}$ are defined in schema (2).

of the intermediate. If the formal potentials were more separated, a double peak in current and in dI/dt curves are also observed (simulations 2 and 3) In variance curves this double peak appears with a relative heigh associated to the color difference among the three colored species.

To corroborate the theory, some real systems are analyzed below.

4. Results and discussion

We show some examples of experimental results of typical adsorbed species on the surface of an electrode with electrochromic properties, or in other words thin films of conducting polymers. Fig. 5 shows experimental results obtained for the study of a PB film in a 0.5 M KCl solution and pH = 3.0. These films were deposited on the ITO transparent electrode and behind the electrode a white patron was placed. Therefore, if PB becomes transparent (ES) the white patron color is observed, if colored, the camera records the color of the PB/ITO/White patron.

In terms of color intensities if the film is as the ES form, a white color is observed (Red, Green and Blue) are high, and if oxidized, Blue coordinate increases, the Red color strongly decreases and the Green color shows a like intermediate behavior, first an increase and after a decrease. Looking at the variance curves, peaks for blue and red colors are clearly separated. It is well-known that voltametric peak for these films should be interpreted as the overlap of at least 3 different processes [8,17].

FdI/dq proves larger at the potentials where the redox process takes place. That means that current measured out of this range of potentials causes no color change and should be attributed to another electrochemical processes, such as catalytic reactions or hydrogen and oxygen

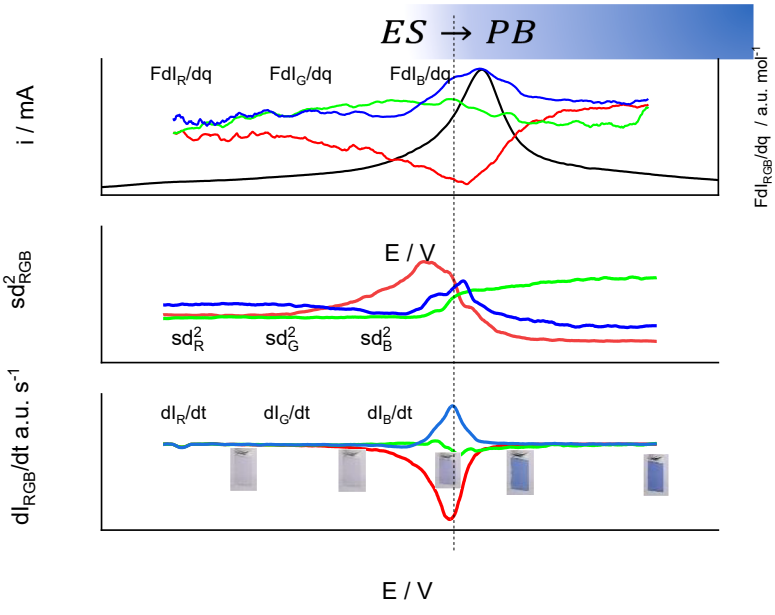

Fig. 5. Example of DVEC plots for PB films on ITO electrodes.

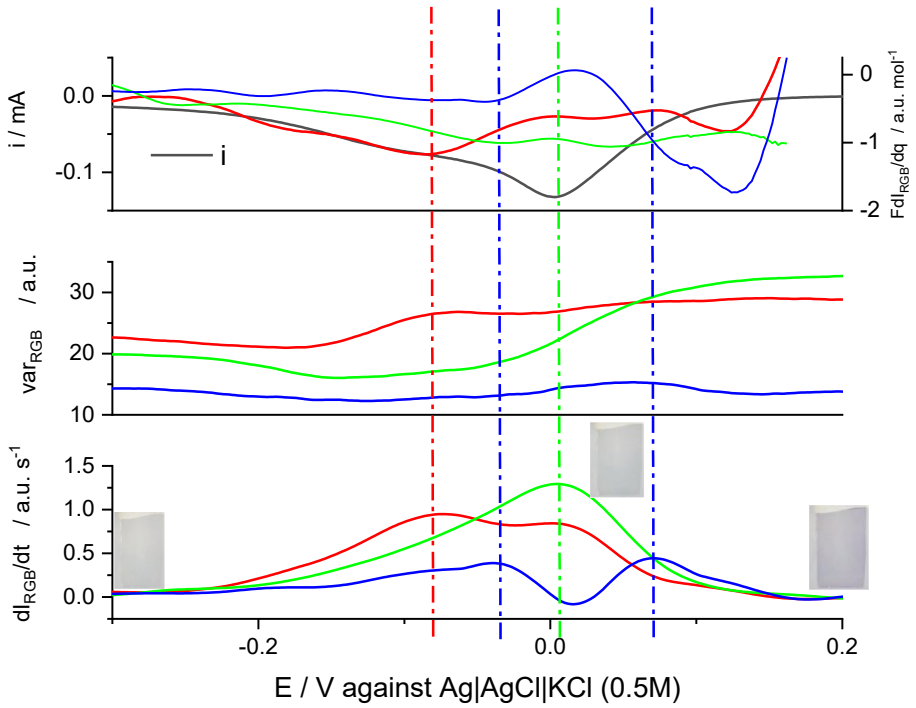

Fig. 6. Example of DVEC plots for PMB films on ITO electrodes. Experimental conditions: pH = 2.2, 0.5M KNO_3 solution. Scan rate 10 mV s^{-1}.

evolution. Notably, FdI/dq for the red color shows the larger absolute values. Finally, the color derivative curves show well-defined peaks for the red and blue coordinates, and out of the range of potentials of the CV peak the baseline for all three color derivatives is zero.

Fig. 6 shows experimental results for another conducting and electrochromic polymer, Poly(methylene Blue), PMB. In this case the reduction voltametric peak is analyzed. This current peak clearly appears of at least a double process. A first well defined voltametric peak (E = 0.05 V) and a secondary process at more negative potentials that appears as a current shoulder (E between −0.085 V and −0.175 V). The derivative for the Green coordinate shows a well-defined peak centered at the first current peak potential. The Red coordinate shows a double peak, one at potentials near the main current peak and the maximum value at the potentials corresponding to the shoulder of the current peak. The Blue coordinate shows a maximum at potentials before the first cathodic peak, then a decrease and finally a second peak before the current shoulder. This behavior shows an evident parallelism with that one of a similar conducting polymer, the poly(azure A)[24,50]. For this case, it has been interpreted as a double electrochemical process with intermediate polaron species. This corresponds to the electrochemical reduction of the intermonomer bridge bonds for the first cathodic process and the monomer reduction for the second one. In this case, this intermediate species appears associated to changes in the Blue color registered for both electroactive centers, the Green color peak could be associated to the bridge electrochemical centers and the second Red process to the monomer electrochemical reduction.

Regarding the FdI/dq curve, one can see that maximum absolute values for the blue coordinate are reached before the first voltametric peak, since at these potentials all the current is associated to the formation of the first intermediate. For the Red color, this absolute maximum is achieved during the reduction of the monomer active center (the current shoulder at potentials near −0.12 V) since at these potentials current associated to the first electrochemical process (the bridge centers) proves very small. For the Green color, FdI/dq reach maximum absolute values at potentials near the first current peak. It should be noted that we are referring color changes to the total current and then, apparent values of this parameter cannot be attributed exclusively to their behavior.

Variance curves for this polymer voltammogram show no more than 15 units of change, that if compared with the PB case of Fig. 5 (100 for the red channel) proves very small. Color intensity derivatives show also very small peaks (1.2 a.u. s^{-1}) or the current peaks (-0.1 mA) while PB peaks reach about 1 mA and $d\bar{I}/dt$ peaks can reach up to 50 a.u. s^{-1}. However, FdI/dq values are on the same order for both systems and then the monochromatic color efficiency should be not very different in PMB and PB. For the PMB case, the film proves clearly less active than PB film, color changes are not very high, but the technique allows to identify as well as current peaks. For the variance curves, it is possible that not all the active centers on the electrode surface are active and then no peak is observed since less than ½ of the centers can change its color.

At this point, it should be considered that the models here presented are only valid for the case of very thin films and reversible (Nernstian) processes since, among others, no transport control has been considered. It is a commonly used simplification for the case of conducting polymers and the current–potential curves are also only valid in these experimental conditions. There are some factors that can modify the shape of experimental curves: ohmic drop that affects the effective potential on the electrode surface, a slow transport of some species which makes the Nernst equation to be not valid on the electrode, the non-reversibility of the electrochemical reaction mechanism, the possible interaction between neighboring electroactive centers, etc. Therefore, if experimental curves do not fit these theoretical models some of these causes can be explored to go beyond the models presented here.

5. Conclusion

Linear sweep voltammetry for electrochromic materials can also be studied by this procedure. In this case, the variance-applied potential curves or the derivative of color intensity-potential curves are directly proportional to the current–potential curves for reversible processes. This fact can allow separating contributions from electrochemical processes associated to different color changes. For the case of very small scan rates, current peaks and derivative of color intensity which are proportional to the scan rate proved very small, but variance curves are

not dependent on this parameter and can be a good alternative to elucidate the mechanism of the surface electrochemical reaction.

Simplified models analyzed in this research represent an ideal situation where color changes from a pure color 1 to a pure color 2. It should also be noted that this model is only valid for thin films, since thicker films can mask color changes of the inner layers. And these are the two main limitations for this methodology.

Analyzing the possibilities one can found that it allows identifying very small color changes such in the case of the poly(methylene blue) here analyzed. Using variance instead of color intensities or absorbance (reflectance) measurements could represent several advantages in some cases. On the one side is that it is possible measuring different rates on different parts of the electrode surface simultaneously.

This methodology can allow to separate different processes and then, a pure response for some overlapped processes could be measured. That represents an advantage in some cases for electroanalysis since it is possible to have the response associated to the main electrochemical reactions without secondary reactions that do not cause color changes for this coordinate, as it could be catalytic reactions, the hydrogen or oxygen evolution reactions or capacitive currents that can mask the obtained result.

Despite we focus our interest on any electrochromic process, this procedure can be extrapolated to any surface process causing color changes. This includes chemical reactions, physical processes, corrosion, degradation of a surface, biological growth, in general any surface process involving color changes.

CRediT authorship contribution statement

Jerónimo Agrisuelas: Conceptualization, Methodology, Writing – review & editing, Data curation. **José Juan García-Jareño:** Conceptualization, Methodology, Writing – review & editing, Data curation. **Francisco Vicente:** Conceptualization, Methodology, Writing – review & editing.

Declaration of Competing Interest

The authors declare that they have no known competing financial interests or personal relationships that could have appeared to influence the work reported in this paper.

Data availability

Data will be made available on request.

Acknowledgement

This work was supported by MINECO-FEDER project CTQ2015-71794-R.

Appendix I. List of symbols

$I_{R,G,B}$: Red, green or blue color intensity of an image pixel.
$\bar{I}_{R,G,B}$: Mean red, green or blue color intensity of the analyzed image.
I_1 or I_2 : characteristic RGB color intensity for the color (1) or color (2) species.
$sd_{R,G,B}$: population standard deviation for RGB color intensities of the analyzed image.
$sd^2_{R,G,B}$: population variance for RGB color intensities of the analyzed image.
n_p : number of pixels of the analyzed image.
n_1 or n_2: number of pixels with color (1) or color (2).
$\Gamma_{red}, \Gamma_{ox}$: surface of concentration of electroactive species.
t : time.
$\omega_{1/2}$: half-peak width for variance and current peaks.
A : Electrode surface area.
R : gas constant.
T : temperature.
F : Faraday's constant.
n : number of electrons.

$$b = \frac{nF}{RT}$$

i : electrical current.
E, E^0, E_s : applied potential, standard potential and starting potential, respectively.
ν : scan rate during a linear sweep voltammetry.

Appendix B. Supplementary data

Supplementary data to this article can be found online at https://doi.org/10.1016/j.microc.2022.107844.

References

[1] A.J. Bard, L.R. Faulkner, Electrochemical Methods: Fundamentals and Applications, 2nd ed., Wiley, New York, 2000.
[2] P.T. Kissinger, W.R. Heineman, Cyclic voltammetry, J. Chem. Educ. 60 (1983) 702, https://doi.org/10.1021/ed060p702.
[3] R.G. Compton, C.E. Banks, Understanding voltammetry, World Sci. (2007), https://doi.org/10.1142/6430.
[4] N. Elgrishi, K.J. Rountree, B.D. McCarthy, E.S. Rountree, T.T. Eisenhart, J. L. Dempsey, A practical beginner's guide to cyclic voltammetry, J. Chem. Educ. 95 (2018) 197–206, https://doi.org/10.1021/acs.jchemed.7b00361.
[5] E. Laviron, Surface linear potential sweep voltammetry: Equation of the peaks for a reversible reaction when interactions between the adsorbed molecules are taken into account, J. Electroanal. Chem. Interfacial Electrochem. 52 (1974) 395–402, https://doi.org/10.1016/S0022-0728(74)80449-3.
[6] J.J. Calvente, R. Andreu, Intermolecular interactions in electroactive thiol monolayers probed by linear scan voltammetry, Curr. Opin. Electrochem. 1 (2017) 22–26, https://doi.org/10.1016/j.coelec.2016.12.006.
[7] M. Yang, R.G. Compton, Voltammetry of adsorbed species: nonideal interactions leading to phase transitions, J. Phys. Chem. C. 124 (2020) 18031–18044, https://doi.org/10.1021/acs.jpcc.0c03791.

[8] B.J. Feldman, O.R. Melroy, Ion flux during electochemical charging of Prussian Blue films, J. Electroanal. Chem. 234 (1987) 213–227.

[9] A.R. Hillman, M.J. Swann, S. Bruckenstein, General-approach to the interpretation of electrochemical quartz crystal microbalance data. 1. Cyclic voltammetry – kinetic subtleties in the electrochemical doping of polybithiophene films, J. Phys. Chem. 95 (1991) 3271–3277.

[10] W. Kutner, K. Doblhofer, Simultaneous cyclic voltammetry and electrochemical quartz-crystal microbalance study at polymer film-modified electrodes of molecular inclusion of ferrocene by beta-cyclodextrin polymer and carboxymethylated beta-cyclodextrin polymer as well as ferrocenecarboxylic acid by beta-cyclodextrin polymer, J. Electroanal. Chem. 326 (1992) 139–160.

[11] C. Gabrielli, M. Keddam, H. Perrot, M.C. Pham, R. Torresi, Separation of ionic and solvent transport during charge compensation processes in electroactive polymers by a.c. electrogravimetry, Electrochimica Acta. 44 (1999) 4217–4225, https://doi.org/10.1016/S0013-4686(99)00136-X.

[12] E. Ventosa, A. Colina, A. Heras, A. Martínez, O. Orcajo, V. Ruiz, J. López-Palacios, Electrochemical, spectroscopic and electrogravimetric detection of oligomers occluded in electrochemically synthesized poly(3,4-ethylenedioxythiophene) films, Electrochimica Acta. 53 (2008) 4219–4227, https://doi.org/10.1016/j.electacta.2007.12.064.

[13] J. Agrisuelas, J.J. García-Jareño, D. Gimenez-Romero, F. Vicente, Innovative combination of three alternating current relaxation techniques: electrical charge, mass, and color impedance spectroscopy. Part I: the tool, J. Phys. Chem. C. 113 (2009) 8430–8437, https://doi.org/10.1021/jp900823z.

[14] D. Ibañez, J. Garoz-Ruiz, A. Heras, A. Colina, Simultaneous UV–visible absorption and raman spectroelectrochemistry, Anal. Chem. 88 (2016) 8210–8217, https://doi.org/10.1021/acs.analchem.6b02008.

[15] P.J. Peerce, A.J. Bard, Polymer films on electrodes: Part III. Digital simulation model for cyclic voltammetry of electroactive polymer film and electrochemistry of poly(vinylferrocene) on platinum, J. Electroanal. Chem. Interfacial Electrochem. 114 (1980) 89–115, https://doi.org/10.1016/S0022-0728(80)80438-4.

[16] J. Heinze, M. Dietrich, Cyclic voltammetry as a tool for characterizing conducting polymers, Mater. Sci. Forum. 42 (1989) 63–78, https://doi.org/10.4028/www.scientific.net/MSF.42.63.

[17] J.J. García-Jareño, J. Navarro-Laboulais, F. Vicente, A numerical approach to the voltammograms of the reduction of Prussian Blue films on ITO electrodes, Electrochimica Acta. 42 (1997) 1473–1480, https://doi.org/10.1016/S0013-4686(96)00302-7.

[18] K. Aoki, K. Tokuda, H. Matsuda, Theory of linear sweep voltammetry with finite diffusion space, J. Electroanal. Chem. 146 (1983) 417–424, https://doi.org/10.1016/S0022-0728(83)80601-9.

[19] J. Agrisuelas, C. Gabrielli, J.J. García-Jareño, D. Gimenez-Romero, J. Gregori, H. Perrot, F. Vicente, Usefulness of F(dm/dQ) function for elucidating the ions role in PB films, J. Electrochem. Soc. 154 (2007) F134–F140, https://doi.org/10.1149/1.2728038.

[20] D. Ellis, M. Eckhoff, V.D. Neff, Electrochromism in the mixed-valence hexacyanides. 1. Voltammetric and spectral studies of the oxidation and reduction of thin-films of prussian blue, J. Phys. Chem. 85 (9) (1981) 1225–1231.

[21] T. Kobayashi, H. Yoneyama, H. Tamura, Electrochemical reactions concerned with electrochromism of polyaniline film-coated electrodes, J. Electroanal. Chem. 177 (1-2) (1984) 281–291.

[22] R.J. Mortimer, 5 Color electrochromicity using prussian blue and nafion/methyl viologen layered films, J. Electrochem. Soc. 138 (1991) 633–634.

[23] P. Kulesza, S. Zamponi, M. Malik, K. Miecznikowski, M. Berrettoni, R. Marassi, Spectroelectrochemical identity of Prussian blue films in various electrolytes: comparison of time-derivative voltabsorptometric responses with conventional cyclic voltammetry, J. Solid State Electrochem. 1 (1997) 88–93.

[24] J. Agrisuelas, D. Giménez-Romero, J.J. García-Jareño, F. Vicente, Vis/NIR spectroelectrochemical analysis of poly-(Azure A) on ITO electrode, Electrochem. Commun. 8 (2006) 549–553, https://doi.org/10.1016/j.elecom.2006.01.022.

[25] E.A. Blubaugh, A.M. Yacynych, W.R. Heineman, Thin-layer spectroelectrochemistry for monitoring kinetics of electrogenerated species, Anal. Chem. 51 (1979) 561–565, https://doi.org/10.1021/ac50040a026.

[26] D.A. Scherson, S. Sarangapani, F.L. Urbach, Thin-layer spectroelectrochemical cell, Anal. Chem. 57 (7) (1985) 1501–1503.

[27] K. Jiao, T. Yang, S. Niu, A thin-layer spectroelectrochemical study of 3,3′,5,5′-tetramethylbenzidine at SnO_2: F film optically transparent electrode, Sci. China Ser. B Chem. 47 (2004) 267–275, https://doi.org/10.1360/03yb0174.

[28] J.J. Garcia-Jareno, D. Gimenez-Romero, F. Vicente, C. Gabrielli, M. Keddam, H. Perrot, EIS and Ac-electrogravimetry study of PB films in KCl, NaCl, and CsCl aqueous solutions, J. Phys. Chem. B. 107 (2003) 11321–11330, https://doi.org/10.1021/jp035387h.

[29] C. Benmouhoub, J. Agrisuelas, N. Benbrahim, F. Pillier, C. Gabrielli, A. Kadri, A. Pailleret, H. Perrot, O. Sel, Influence of the Incorporation of CeO2 nanoparticles on the ion exchange behavior of dodecylsulfate doped polypyrrole films: ac-electrogravimetry investigations, Electrochimica Acta. 145 (2014) 270–280, https://doi.org/10.1016/j.electacta.2014.07.151.

[30] V.M. Huang, S.-L. Wu, M.E. Orazem, N. Pébère, B. Tribollet, V. Vivier, Local electrochemical impedance spectroscopy: A review and some recent developments, Electrochimica Acta. 56 (2011) 8048–8057, https://doi.org/10.1016/j.electacta.2011.03.018.

[31] O. Gharbi, K. Ngo, M. Turmine, V. Vivier, Local electrochemical impedance spectroscopy: A window into heterogeneous interfaces, Curr. Opin. Electrochem. 20 (2020) 1–7, https://doi.org/10.1016/j.coelec.2020.01.012.

[32] J. Garoz-Ruiz, A. Heras, A. Colina, Simultaneous study of different regions of an electrode surface with a novel spectroelectrochemistry platform, Electrochem. Commun. 90 (2018) 73–77, https://doi.org/10.1016/j.elecom.2018.04.006.

[33] J. Agrisuelas, J.J. García-Jareño, E. Perianes, F. Vicente, Use of RGB digital video analysis to study electrochemical processes involving color changes, Electrochem. Commun. 78 (2017) 38–42, https://doi.org/10.1016/j.elecom.2017.04.001.

[34] J. Agrisuelas, J.J. García-Jareño, F. Vicente, Quantification of electrochromic kinetics by analysis of RGB digital video images, Electrochem. Commun. 93 (2018) 86–90, https://doi.org/10.1016/j.elecom.2018.06.011.

[35] J. Agrisuelas, J.J. García-Jareño, E. Guillén, F. Vicente, Kinetics of surface chemical reactions from a digital video, J. Phys. Chem. C. 124 (2020) 2050–2059, https://doi.org/10.1021/acs.jpcc.9b10689.

[36] J. Agrisuelas, J.J. García-Jareño, F. Vicente, Evaluating the practical use of digital video to study the effect of sheet resistance of transparent indium-tin oxide electrodes using the galvanostatic deposition of poly(o-toluidine), J. Electrochem. Soc. 165 (2018) G101–G107, https://doi.org/10.1149/2.1021809jes.

[37] J. Agrisuelas, J.J. García-Jareño, E. Guillén, F. Vicente, RGB video electrochemistry of copper electrodeposition/electrodissolution in acid media on a ternary graphite: copper:polypropylene composite electrode, Electrochimica Acta. 305 (2019) 72–80, https://doi.org/10.1016/j.electacta.2019.03.016.

[38] E. Guillén, M. Ferrer-Roselló, J. Agrisuelas, J.J. García-Jareño, F. Vicente, Digital video-electrochemistry (DVEC) to assess electrochromic materials in the frequency domain: RGB colorimetry impedance spectroscopy, Electrochimica Acta. 366 (2021), 137340, https://doi.org/10.1016/j.electacta.2020.137340.

[39] M. Vidal, J.M. Amigo, R. Bro, F. van den Berg, M. Ostra, C. Ubide, Image analysis for maintenance of coating quality in nickel electroplating baths – Real time control, Anal. Chim. Acta. 706 (2011) 1–7, https://doi.org/10.1016/j.aca.2011.08.007.

[40] M. Vidal, J.M. Amigo, R. Bro, M. Ostra, C. Ubide, J. Zuriarrain, Flatbed scanners as a source of imaging. Brightness assessment and additives determination in a nickel electroplating bath, Anal. Chim. Acta. 694 (2011) 38–45, https://doi.org/10.1016/j.aca.2011.03.030.

[41] K. Thajee, P. Paengnakorn, W. Wongwilai, K. Grudpan, Application of a webcam camera as a cost-effective sensor with image processing for dual electrochemical – colorimetric detection system, Talanta. 185 (2018) 160–165, https://doi.org/10.1016/j.talanta.2018.03.055.

[42] L. Furnell, P.J. Holliman, A. Connell, E.W. Jones, R. Hobbs, C.P. Kershaw, R. Anthony, J. Searle, T. Watson, J. McGettrick, Digital imaging to simultaneously study device lifetimes of multiple dye-sensitized solar cells, Sustain Energy Fuels 1 (2017) 362–370, https://doi.org/10.1039/C7SE00015D.

[43] J. Agrisuelas, J. García-Jareño, D. Gimenez-Romero, F. Negrete, F. Vicente, The fractal dimension as estimator of the fractional content of metal matrix composite materials, J. Solid State Electrochem. 13 (2009) 1599–1603, https://doi.org/10.1007/s10008-008-0743-8.

[44] D. Giménez-Romero, J.J. García-Jareño, F. Vicente, Correlation between the fractal dimension of the electrode surface and the EIS of the zinc anodic dissolution for different kinds of galvanized steel, Electrochem. Commun. 6 (2004) 148–152, https://doi.org/10.1016/j.elecom.2003.11.003.

[45] J. Agrisuelas, J.J. García-Jareño, F. Vicente, Spatiotemporal colorimetry to reveal electrochemical kinetics of poly(o-toluidine) films along ITO surface, Electrochimica Acta. 269 (2018) 350–358, https://doi.org/10.1016/j.electacta.2018.02.157.

[46] K. Itaya, T. Ataka, S. Toshima, Spectroelectrochemistry and electrochemical preparation method of Prussian blue modified electrodes, J. Am. Chem. Soc. 104 (1982) 4767–4772, https://doi.org/10.1021/ja00382a006.

[47] A. Roig, J. Navarro, J.J. Garcia, F. Vicente, Voltammetric study of the stability of deposited Prussian blue films against succesive potential cycling, Electrochimica Acta. 39 (1994) 437–442, https://doi.org/10.1016/0013-4686(94)80083-9.

[48] R. Pauliukaite, C.M.A. Brett, Poly(neutral red): electrosynthesis, characterization, and application as a redox mediator, Electroanalysis. 20 (2008) 1275–1285, https://doi.org/10.1002/elan.200804217.

[49] F. Huang, A. Sugimoto, Image and Video Technology – PSIVT 2013 Workshops: GCCV 2013, GPID 2013, PAESNPR 2013, and QACIVA 2013, Guanajuato, Mexico, October 28–29, 2013, Revised Selected Papers, Springer, 2014.

[50] E. Guillén, J. Agrisuelas, J.J. García-Jareño, F. Vicente, Electrochromic Performances of Poly(Azure A) Films from Digital Video-Electrochemistry (DVEC), J. Electrochem. Soc. 167 (2020), 106514, https://doi.org/10.1149/1945-7111/ab9e3b.

[51] L. Roullier, E. Laviron, Effect of uncompensated ohmic drop in surface linear potential sweep voltammetry: application to the determination of surface rate constants, J. Electroanal. Chem. Interfacial Electrochem. 157 (1983) 193–203, https://doi.org/10.1016/S0022-0728(83)80350-7.

[52] P.R. Bueno, D. Giménez-Romero, F.F. Ferreira, G.O. Setti, J.J. Garcia-Jareño, J. Agrisuelas, F. Vicente, Electrochromic Switching Mechanism of Iron Hexacyanoferrates Molecular Compounds: The Role of Fe2+(CN)6 Vacancies, J. Phys. Chem. C. 113 (2009) 9916–9920, https://doi.org/10.1021/jp901146w.